Methods in Molecular Biology 2064

Springer Protocols

Bindesh Shrestha *Editor*

Single Cell Metabolism

Methods and Protocols

Humana Press

METHODS IN MOLECULAR BIOLOGY

Series Editor
John M. Walker
School of Life and Medical Sciences
University of Hertfordshire
Hatfield, Hertfordshire, UK

For further volumes:
http://www.springer.com/series/7651

For over 35 years, biological scientists have come to rely on the research protocols and methodologies in the critically acclaimed *Methods in Molecular Biology* series. The series was the first to introduce the step-by-step protocols approach that has become the standard in all biomedical protocol publishing. Each protocol is provided in readily-reproducible step-by-step fashion, opening with an introductory overview, a list of the materials and reagents needed to complete the experiment, and followed by a detailed procedure that is supported with a helpful notes section offering tips and tricks of the trade as well as troubleshooting advice. These hallmark features were introduced by series editor Dr. John Walker and constitute the key ingredient in each and every volume of the *Methods in Molecular Biology* series. Tested and trusted, comprehensive and reliable, all protocols from the series are indexed in PubMed.

Single Cell Metabolism

Methods and Protocols

Edited by

Bindesh Shrestha

Waters Corporation, Milford, MA, USA

Humana Press

Editor
Bindesh Shrestha
Waters Corporation
Milford, MA, USA

ISSN 1064-3745 ISSN 1940-6029 (electronic)
Methods in Molecular Biology
ISBN 978-1-4939-9829-6 ISBN 978-1-4939-9831-9 (eBook)
https://doi.org/10.1007/978-1-4939-9831-9

Chapter 11

Toward Single Cell Molecular Imaging by Matrix-Free Nanophotonic Laser Desorption Ionization Mass Spectrometry

Sylwia A. Stopka and Akos Vertes

Abstract

In recent years, innovations in mass spectrometry imaging (MSI) have enabled simultaneous detection and mapping of biomolecules and xenobiotics directly from biological tissues and single cells. Matrix-assisted laser desorption ionization (MALDI) has been the most widely embraced MSI technique. However, this technique can exhibit ion suppression effects hindering metabolite coverage and possesses a narrow dynamic range. Nanophotonic platforms, e.g., silicon nanopost array (NAPA) structures, can be used as an alternative for matrix-free imaging of biological tissues. Here, we present a protocol for MSI of large and small adherent cell clusters by laser desorption ionization from NAPA with minimal sample preparation.

Key words Mass spectrometry imaging, Cell culture, Cell clusters, Metabolites, Nanopost array, NAPA, Molecular imaging

1 Introduction

The stochastic nature of gene and protein expression results in cellular heterogeneity within complex biological tissues, and can also manifest in fluctuations of metabolite levels [1]. To capture a true snapshot of the molecular composition of a single cell with minimum perturbation, technological advancements are needed. Mass spectrometry (MS) is a promising tool for the detection, quantification, and identification of an array of biomolecules. However, general MS measurements of biological tissues include bulk measurements that mask individual cell signals, or require sample preparation, which obscures the spatial information for molecular distributions. To overcome these challenges, MS imaging (MSI) techniques have been introduced based on, for example, matrix-assisted laser desorption ionization (MALDI) [2, 3]. Over the years, improvements in sensitivity and lateral resolution have made it possible to perform tissue imaging with cellular resolution

Bindesh Shrestha (ed.), *Single Cell Metabolism: Methods and Protocols*, Methods in Molecular Biology, vol. 2064,
https://doi.org/10.1007/978-1-4939-9831-9_11,

and capture the spatial distributions for an array of biomolecules, e.g., metabolites, lipids, proteins, and xenobiotics, from single cells [4, 5]. However, spectral interferences and ion suppression are sometimes observed due to the application of the matrix, hindering small molecule analysis [6]. Quantitation by MALDI-MSI also remains a challenge because of the limited dynamic range of the MALDI signal.

Several emerging matrix-free platforms have demonstrated successful MSI of small molecules from biological tissues using laser deposition ionization LDI [7]. These ionization sources rely on the interaction between the laser radiation and a nanostructure to induce LDI. Among these only a few have been demonstrated for MSI, including desorption ionization on porous silicon (DIOS) [8], nanostructure initiator mass spectrometry (NIMS) [9–11] and silicon nanopost array (NAPA) platforms [12–14]. Due to the exquisite sensitivity and dynamic range exhibited by these ionization sources for small molecule analysis, detection of metabolites in single yeast cells was achieved [15, 16]. Furthermore, these silicon structures can be a promising substrate for culturing cells and microfluidics applications.

Over the years, biocompatible materials have gained increasing interest. For example, porous silicon possesses unique chemical and physical properties that are conducive for use as a substrate for cell growth [17, 18]. Silicon is often used in biosensors, as a substrate in lab-on-a-chip designs or as tissue engineering scaffolds [19–22]. Silicon nanostructure arrays have also been used to investigate cellular morphology, and can be tuned to capture circuiting tumor cells [23, 24].

Adherent mammalian cells can be a model system to study human diseases, drug interactions, and cellular heterogeneity in situ [25–27]. However, current practices for handling these cells include cell lysis and enzymatic digestion, which may alter their biochemical composition and rely on bulk measurements. In this contribution, we present a protocol that uses silicon NAPA as a platform for culturing the cells and MSI with minimal cell manipulation.

2 Materials

2.1 Reagents and Chemicals

1. Cell culture medium consists of Eagle's Minimum Essential Medium (EMEM) (30-2003; ATCC, Manassas, VA) supplemented with 10% fetal bovine serum (FBS) (30-2020; ATCC, Manassas, VA) and 1% Penicillin-streptomycin (ThermoFisher, Waltham, MA).
2. Trypsin-EDTA (0.25%) (ThermoFisher, Waltham, MA) for cell detachment.

3. Trypan blue solution (0.4%) (ThermoFisher, Waltham, MA) for cell counting.
4. 70% ethanol can be used to sterilize the NAPA chip.

2.2 Biological Samples and Equipment

1. Cryogenic stock of human hepatocarcinoma cells (HepG2/C3A; CRL-10741, ATCC, Manassas, VA) derived from liver (*see* **Note 1**).
2. A humidity-controlled cell incubator (HeraCell; Thermo Scientific, Waltham, MA) that operates at a constant 5% CO_2 and 37 °C.
3. Automated cell counter (Countess; Invitrogen, Eugene, OR).
4. 35 cm diameter polystyrene Petri culture dishes.
5. Optical microscope with DIC option and scanning electron microscope.

2.3 NAPA Imaging Chips

1. Patterning for nanofabrication of the NAPA substrate is performed on low resistivity p-type silicon wafers by either e-beam lithography (EBL) or deep UV projection lithography (DUV-PL). The former is a much lengthier process and is not conducive to making large area NAPA imaging chips.
2. Both fabrication methods of the silicon NAPA are described in detail in our previous work [12, 28].
3. Briefly, for DUV-PL a layer of SiO_2 is developed by thermal oxidation followed by spin coating a negative tone photoresist. The wafer then undergoes DUV-PL exposure at 248 nm wavelength to create the nanopost pattern.
4. The photoresist is then developed and the exposed SiO_2 is etched away to form a hard mask for the nanoposts.
5. The remaining photoresist is striped, leaving only a layer of SiO_2 hard mask protecting the positions of the nanoposts. Using a mixture of etchant gases, the silicon surrounding the nanoposts is etched away in a deep reactive ion etching (DRIE) process.
6. The fabricated nanoposts are 1000 nm in height, 150 nm in diameter, and 337 nm in periodicity. The NAPA imaging chips were produced to a size of 4×4 mm^2 to accommodate biological tissue sections.

2.4 Mass Spectrometer and Supplies

1. Oil-free vacuum desiccator system (813-600; Ted Pella, Inc., Redding, CA) to dry the sample on the NAPA chip prior to analysis.
2. Dry box for NAPA storage.
3. Double-sided carbon tape to mount the chips onto a MALDI plate (*see* **Note 2**).

4. A linear ion trap-orbitrap hybrid mass spectrometer fitted with a MALDI ion source (MALDI LTQ-Orbitrap XL; Thermo Fisher Scientific Inc., Bremen, Germany) can be used for NAPA-LDI-MSI experiments. Ion assignments are facilitated by tandem MS (MS/MS). The nitrogen laser within the source operates at a wavelength and repetition rate of 337 nm and 60 Hz, respectively.

2.5 Software

1. Xcalibur (3.0.63) (ThermoFisher Scientific Inc., Bremen, Germany) for the interpretation of mass spectra.
2. ImageQuest (1.1.0) (ThermoFisher Scientific Inc., Bremen, Germany) for molecular image processing and the reconstruction of chemical images.

3 Methods

3.1 Culturing of Mammalian Cells on NAPA Substrates

1. A stock of HepG2/C3A cells should be maintained by culturing them in a T75 flask in the supplemented EMEM medium. Grow the cells till 70–80% confluence. To detach the cells from the flask surface, aspirate the medium out completely, wash with 1× PBS, aspirate the PBS solution, and add 4 mL of pre-warmed trypsin EDTA (Fig. 1(1)).
2. Place the flask into the humidity-controlled incubator for 10 min for the digestion of the extracellular matrix to be complete; tap the flask gently to insure cell detachment.
3. Deactivate the trypsin with the addition of fresh pre-warmed EMEM media and centrifuge ($1000 \times g$) the cell suspension to form a cell pellet (Fig. 1(2)). Aspirate the trypsin and medium solution from the cells and resuspend the cell pellet with 2 mL of fresh medium.
4. To avoid cell clumping, gently aspirate the cell suspension up and down ten times with a pipette.
5. Measure the cell density by mixing, the cell suspension and trypan blue solution 1:1 (v/v) and use a cell counter to measure the cell numbers. Dilute the cell suspension to ~5×10^4 cells/mL.
6. Sterilize a 4×4 mm^2 NAPA chip with 70% ethanol and place the chip in a 35 mm culture dish.
7. Pipet 15 μL of the diluted cell suspension onto the NAPA chip, resulting in a seeding density of ~750 cells per 4×4 mm^2 NAPA chip (Fig. 1(3)).
8. Place the NAPA chip covered by the cells in the incubator for 15 min to allow the cells to adhere to the silicon substrate.

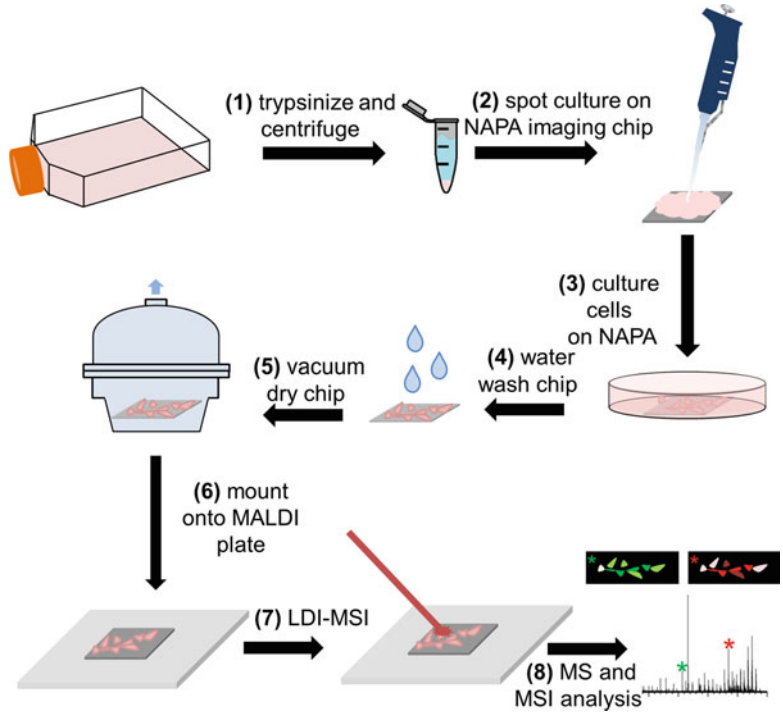

Fig. 1 Workflow of sample preparation and MSI analysis for mammalian cells cultured on NAPA imaging chips. A flask of hepatocarcinoma cells is first (1) trypsinized to detach the cells from the flask followed by centrifugation to form a cell pellet. (2) The cell pellet is then dispensed onto the NAPA structure and (3) cultured for six days. Once the cells are ready for analysis, the NAPA chip is (4) water washed, (5) vacuumed dried, and (6) affixed onto a standard MALDI plate for MSI. (7) Imaging experiments are performed by rastering over the cultured cells with a laser with mass spectra acquired at every pixel. Molecular images (8) are constructed from the MSI experiment by plotting ion intensity distributions for biomolecules directly from the cultured cells

9. Gently fill the 35 mm dish containing the NAPA chips with ¾ EMEM medium and place them in the incubator. Change out the medium every other day and monitor the cell growth daily using optical microscopy (Fig. 1(3)).

3.2 Sample Preparation for LDI-MSI

1. After 6 days of culturing the cells on the NAPA structure, remove the chips from the Petri dish with tweezers. Rotate the chip to vertical orientation and gently wash it with water to remove any excess media (*see* **Note 3**) (Fig. 1(4)).
2. Place the NAPA chips containing the cells inside an oil-free vacuum desiccator (at ~75 Torr pressure) for 10 min for the cells to dry on the NAPA substrate (Fig. 1(5)).
3. Throughout culturing, washing, and vacuum drying, the cells should be inspected using optical microscopy to insure that

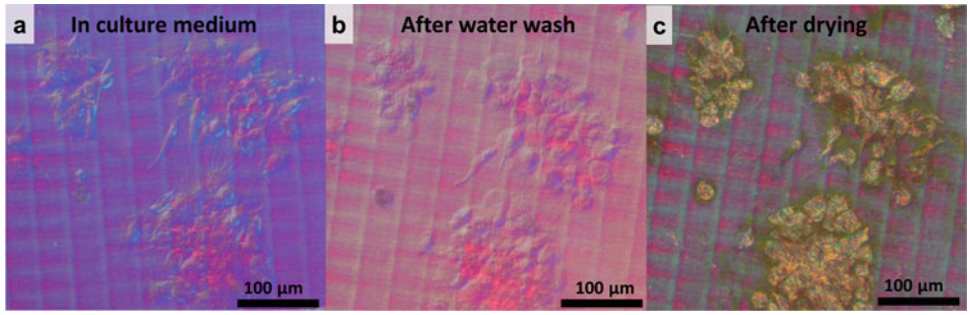

Fig. 2 Optical images of the HepG2C3A cells cultured on NAPA substrate in (**a**) culturing medium, (**b**) after a gentle water wash, and (**c**) after drying the cells for analysis

their morphology is unchanged and no physical damage has been inflicted (Fig. 2a–c).

4. Once the NAPA chip is dry, using a double-sided carbon tape, affix it to a standard MALDI plate (Fig. 1(6)) and insert it into the mass spectrometer for LDI-MSI acquisition (Fig.1(7, 8)).

3.3 Optimization of NAPA-MSI Signal

1. To obtain robust and stable signal during the MSI run, several parameters need to be optimized on a test NAPA chip that has undergone similar sample preparation steps and contains adherent cells.
2. Since these are imaging experiments and the ions are collected as discrete packets at each pixel, the automatic gain control (AGC) feature is turned off.
3. The laser energy for MSI experiments should be optimized by firing varied fluences directly on the cell cluster surface ranging from 60 to 100 mJ/cm^2 (*see* **Note 4**). Optimization of the NAPA-MSI signal is complete when its intensity is the highest and in-source fragmentation is at the minimum.
4. The number of laser shots per pixel should be configured, as well. Once the laser fluence is optimized, adjust the number of shots between 2 and 10 per pixel. Once again select the configuration that provides the best signal.
5. Lastly, for cell cluster imaging a spatial resolution of <50 µm is recommended; based on the laser spot size in the mass spectrometer, oversampling maybe required. In this protocol, the laser spot size is 100 × 80 µm^2, thus oversampling may be needed.
6. Mass resolving power can be varied between $R = 30{,}000$ and 100,000 and its selection is dictated by the application. Longer acquisition times and loss in sensitivity can be expected at higher resolving powers.

3.4 NAPA Imaging

1. In order to obtain molecular images by LDI from NAPA, mass spectra are collected for all the pixels that are later rendered as false color images based on the ion intensities. A motorized stage translates the sample in two dimensions to obtain a mass spectrum at each pixel. Below are the steps for obtaining the molecular images.
2. Scan the region of interest, in this case the whole 4×4 mm^2 NAPA chip, to produce the optical image needed for co-registration.
3. Input the optimal experimental parameters for the number of laser shots per pixel, laser fluence, and step size (e.g., 50 μm).
4. Start the MSI data acquisition.
5. Once the analysis is complete, place the instrument in standby mode.

3.5 Data Processing and Inspection of Cells After LDI

1. Using the Xcalibur software, all of the pixels from the NAPA area are averaged to show the overall signal quality (Fig. 3). In both positive and negative ion modes, small metabolites and lipid species are detected from the adherent HepG2/C3A cells.
2. (Optional) Using SEM, the NAPA chips are inspected before and after LDI-MSI (Fig. 4). Prior to laser irradiation, the cells, including their lamellipodia, are attached to the silicon substrate (Fig. 4a).

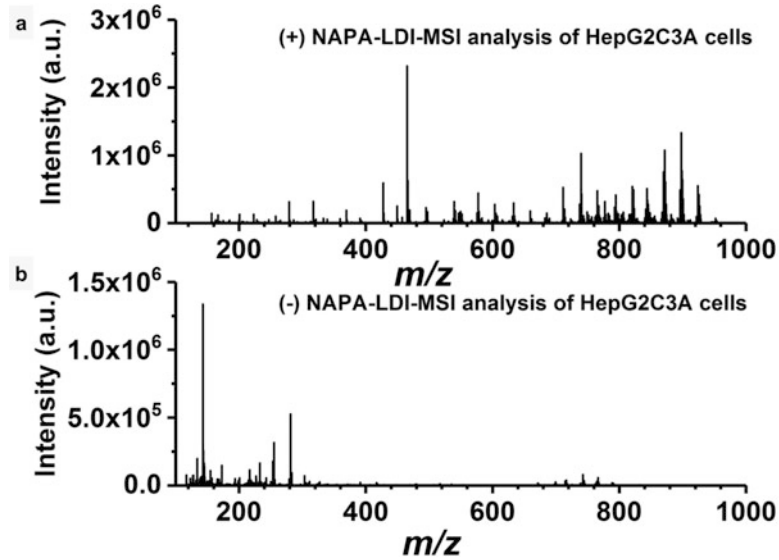

Fig. 3 Averaged mass spectra for HepG2C3A cells cultured directly on a NAPA substrate in (**a**) positive and (**b**) negative ion modes. Small metabolites and lipids are detected

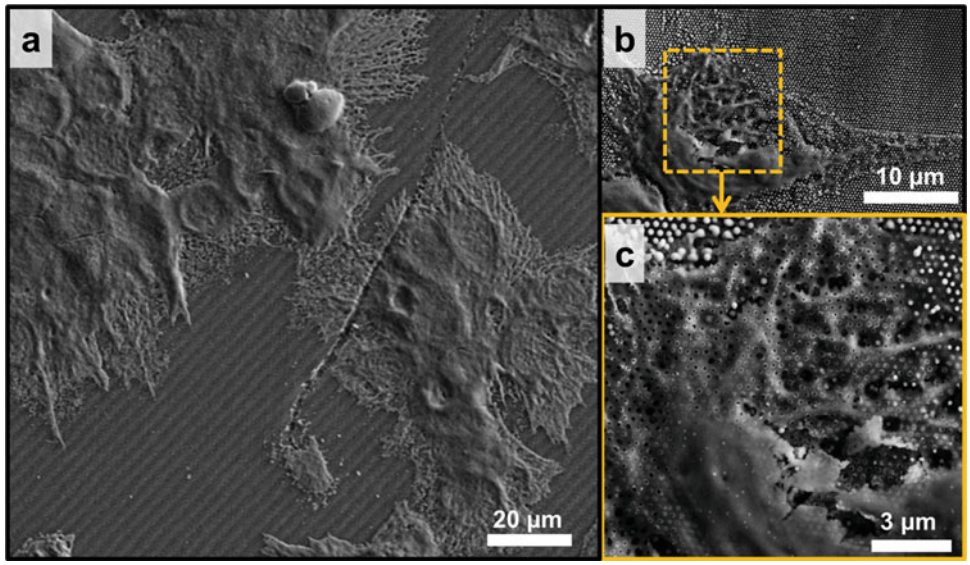

Fig. 4 (**a**) An SEM image of cells attached to the NAPA surface before LDI analysis. (**b**) After LDI analysis, SEM images revealed desorption of cellular material due to laser irradiation. (**c**) Zoomed-in region shows nanopores in the cell material that are similar in diameter and periodicity to the underlying NAPA posts

3. (Optional) After laser exposure, a zoomed in SEM image shows that cellular material is removed in the LDI process (Fig. 4b). Closer inspection of the exposed cell indicates a pattern of nanopores that follows the nanopost positions, indicating the role of nanopost heating in material desorption (Fig. 4c).

3.6 Large Cell Population Imaging

1. A cell population containing ~2000 adherent cells on a NAPA chip can be analyzed.
2. Prior to LDI-MSI, the dried NAPA chip is imaged using optical microscopy to locate the cell clusters (Fig. 5a).
3. To produce molecular images based on ion intensities, the whole NAPA chip is rastered using 50 μm step size. This results in a total of 6724 pixels to form images based on the ion intensities for particular *m/z* values at each pixel.
4. A few hundred biomolecules can be detected and their ion intensities can be spatially mapped to show their localization within the whole cell population (Fig. 5b, c). For example, the distributions of $[\text{glutathione} + \text{K}]^+$ and $[\text{cholesterol} + \text{H-H}_2\text{O}]^+$ are observed throughout the whole cell population.
5. Background ions from the NAPA chip can also be spatially mapped (*see* the blue composite image in Fig. 5d).
6. The images of these two biomolecules and the NAPA background ions can be overlaid to observe their distributions in relation to each other (Fig. 5e).

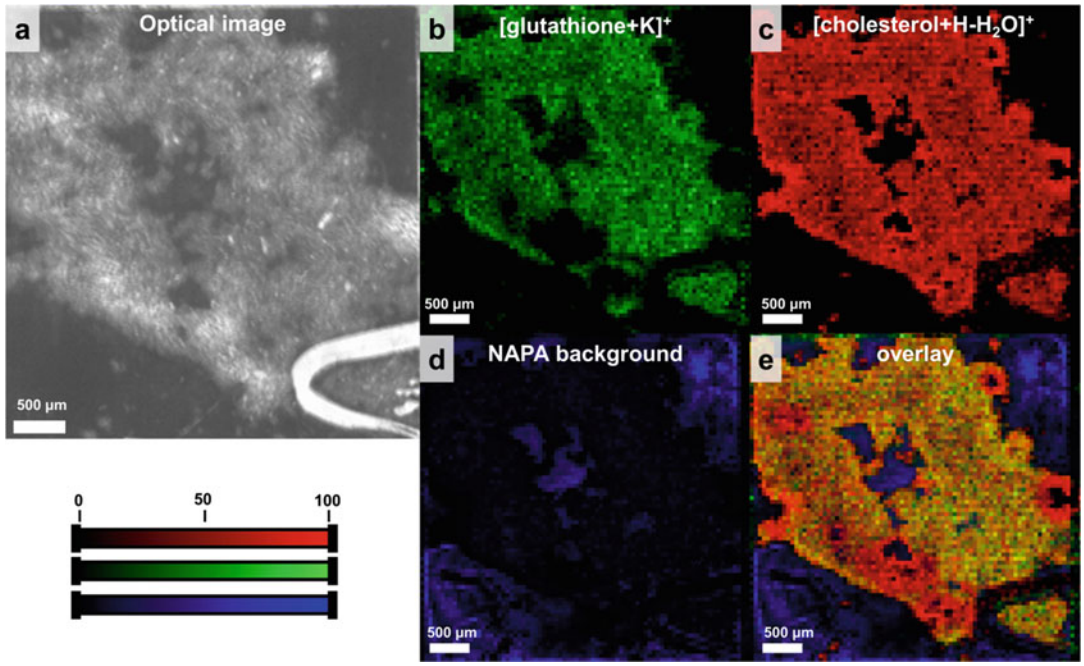

Fig. 5 (**a**) Optical image from mass spectrometer camera of NAPA imaging chip containing ~2000 HepG2/C3A cells. Molecular images based on metabolite ion intensities, e.g., (**b**) glutathione and (**c**) cholesterol can be spatially correlated with the location of cell clusters. Selection of (**d**) NAPA-related background peaks can reveal the exposed NAPA substrate. (**e**) Superimposed molecular images reveal overlaying spatial distributions from the cell clusters as well as the NAPA substrate

3.7 Small Cell Cluster Imaging

1. Regions of interest from the co-registered optical and molecular images can be selected to show the distribution of biomolecules from small cell clusters (Fig. 6).
2. Using the optical image the number of adherent cells can be counted for each small cell cluster.
3. Molecular images can be used to assess the signal and the resolution of spatial mapping based on the pixels corresponding to cell clusters.
4. Several metabolites and lipids can be localized to clusters of ~10 cells. For example, $[\text{phosphocholine}]^+$, $[\text{PE}(36{:}2) + \text{K}]^+$, $[\text{TG}(54{:}3) + \text{K}]^+$, and $[\text{glutathione} + \text{K}]^+$ were all detected in the small cell clusters (Fig. 6b–e).
5. Clusters of $n < 10$ cells result in no signal, indicating that the sensitivity of this LDI platform is reached. However, surface silanization or use of bowtie configured NAPA posts can improve ionization efficiency and could ultimately be used for single cell analysis.

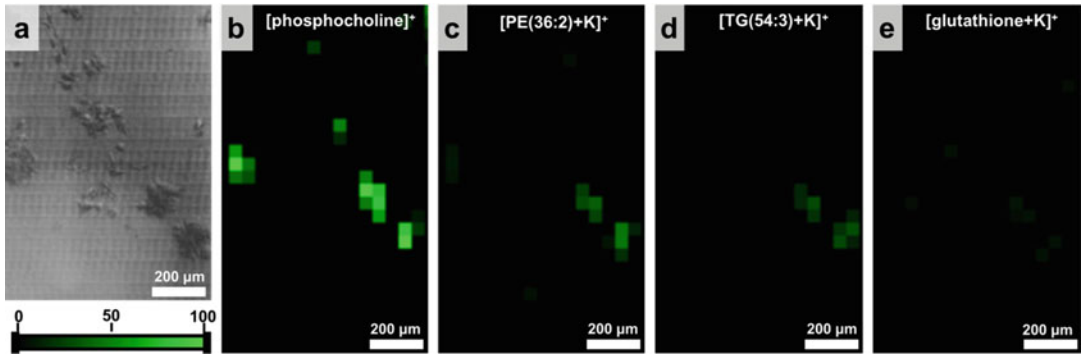

Fig. 6 (**a**) Optical image of small cell clusters attached to NAPA substrate. (**b**–**e**) Corresponding molecular images of small metabolites and lipid species detected from the cell clusters. Signal was only observed in cell clusters of $n = 10$ or larger

4 Notes

1. The HepG2/C3A cells require biosafety level one (BSL-1) environment and all cell handling and culturing should be performed in a BLS-1 rated hood. All equipment and instruments that may come in contact with the cells should have biohazard sign posted.
2. Depending on the type of mass spectrometer, make sure there is enough clearance for the carbon tape and NAPA chip to be inserted into the instrument.
3. When pipetting directly onto the NAPA chips, avoid touching the nanostructure with the pipette tip. Touching the surface will damage the posts, resulting in poor signal within that area. For example, in Fig. 5 the lower right corner of the chip was damaged with a pipette tip and poor signal in that area can be seen in the molecular images.
4. Due to the rapid heating of the nanoposts, in-source fragmentation of labile compounds is observed. To minimize this effect, use lower laser fluences. Direct analysis of a standard compound mixture can be used to assess the amount of in-source fragmentation for those specific compounds.

Acknowledgments

Research was sponsored by the U.S. Army Research Office and the Defense Advanced Research Projects Agency and was accomplished under Cooperative Agreement Number W911NF-14-2-0020. The views and conclusions contained in this document are those of the authors and should not be interpreted as representing the official policies, either expressed or implied, of the Army Research Office,

DARPA, or the U.S. Government. The U.S. Government is authorized to reproduce and distribute reprints for Government purposes notwithstanding any copyright notation hereon.

References

1. Taniguchi Y (2011) Quantifying *E. coli* proteome and transcriptome with single-molecule sensitivity in single cells (vol. 329, p. 533, 2010). Science 334(6055):453–453
2. Caprioli RM (2014) Imaging mass spectrometry: molecular microscopy for enabling a new age of discovery. Proteomics 14 (7–8):807–809. https://doi.org/10.1002/pmic.201300571
3. McDonnell LA, Heeren RMA (2007) Imaging mass spectrometry. Mass Spectrom Rev 26 (4):606–643. https://doi.org/10.1002/mas.20124
4. Zavalin A, Yang JH, Caprioli R (2013) Laser beam filtration for high spatial resolution MALDI imaging mass spectrometry. J Am Soc Mass Spectrom 24(7):1153–1156. https://doi.org/10.1007/s13361-013-0638-5
5. Schuerenberg M, Luebbert C, Deininger SO, Ketterlinus R, Suckau D (2007) MALDI tissue imaging: mass spectrometric localization of biomarkers in tissue slices. Nat Methods 4(5): iii–iiv
6. Ferguson CN, Fowler JWM, Waxer JF, Gatti RA, Loo JA (2014) Mass spectrometry-based tissue imaging of small molecules. In: Woods AG, Darie CC (eds) Advancements of mass spectrometry in biomedical research, vol 806. Advances in experimental medicine and biology. Springer, New York, NY, pp 283–299. https://doi.org/10.1007/978-3-319-06068-2_12
7. Bergman N, Shevchenko D, Bergquist J (2014) Approaches for the analysis of low molecular weight compounds with laser desorption/ionization techniques and mass spectrometry. Anal Bioanal Chem 406 (1):49–61. https://doi.org/10.1007/s00216-013-7471-3
8. Wei J, Buriak JM, Siuzdak G (1999) Desorption-ionization mass spectrometry on porous silicon. Nature 399(6733):243–246. https://doi.org/10.1038/20400
9. Northen TR, Yanes O, Northen MT, Marrinucci D, Uritboonthai W, Apon J, Golledge SL, Nordstrom A, Siuzdak G (2007) Clathrate nanostructures for mass spectrometry. Nature 449(7165):1033–U1033. https://doi.org/10.1038/nature06195
10. Patti GJ, Shriver LP, Wassif CA, Woo HK, Uritboonthai W, Apon J, Manchester M, Porter FD, Siuzdak G (2010) Nanostructure-initiator mass spectrometry (NIMS) imaging of brain cholesterol metabolites in Smith-Lemli-Opitz syndrome. Neuroscience 170 (3):858–864. https://doi.org/10.1016/j.neuroscience.2010.07.038
11. Greving MP, Patti GJ, Siuzdak G (2011) Nanostructure-initiator mass spectrometry metabolite analysis and imaging. Anal Chem 83(1):2–7. https://doi.org/10.1021/ac101565f
12. Walker BN, Stolee JA, Pickel DL, Retterer ST, Vertes A (2010) Tailored silicon nanopost arrays for resonant nanophotonic ion production. J Phys Chem C 114(11):4835–4840. https://doi.org/10.1021/jp9110103
13. Stopka SA, Rong C, Korte AR, Yadavilli S, Nazarian J, Razunguzwa TT, Morris NJ, Vertes A (2016) Molecular imaging of biological samples on nanophotonic laser desorption ionization platforms. Angew Chem Int Ed 55 (14):4482–4486. https://doi.org/10.1002/anie.201511691
14. Fincher JA, Dyer JE, Korte AR, Yadavilli S, Morris NJ, Vertes A (2018) Matrix-free mass spectrometry imaging of mouse brain tissue sections on silicon nanopost arrays. J Comp Neurol 25(10):24566
15. Walker BN, Antonakos C, Retterer ST, Vertes A (2013) Metabolic differences in microbial cell populations revealed by nanophotonic ionization. Angew Chem Int Ed 52 (13):3650–3653. https://doi.org/10.1002/anie.201207348
16. Walker BN, Stolee JA, Vertes A (2012) Nanophotonic ionization for ultratrace and single-cell analysis by mass spectrometry. Anal Chem 84(18):7756–7762. https://doi.org/10.1021/ac301238k
17. Unal B (2011) Quenching influence of cell culture medium on photoluminescence and morphological structure of porous silicon. Appl Surf Sci 258(1):207–211. https://doi.org/10.1016/j.apsusc.2011.08.032
18. Bhuyan MK, Rodriguez-Devora JI, Fraser K, Tseng TLB (2014) Silicon substrate as a novel cell culture device for myoblast cells. J Biomed

Sci 21. https://doi.org/10.1186/1423-0127-21-47

19. Alvarez SD, Derfus AM, Schwartz MP, Bhatia SN, Sailor MJ (2009) The compatibility of hepatocytes with chemically modified porous silicon with reference to in vitro biosensors. Biomaterials 30(1):26–34. https://doi.org/10.1016/j.biomaterials.2008.09.005
20. Lehto V-P, Vähä-Heikkilä K, Paski J, Salonen J (2005) Use of thermoanalytical methods in quantification of drug load in mesoporous silicon microparticles. J Therm Anal Calorim 80 (2):393–397. https://doi.org/10.1007/s10973-005-0666-x
21. Temiz Y, Lovchik RD, Kaigala GV, Delamarche E (2015) Lab-on-a-chip devices: how to close and plug the lab? Microelectron Eng 132:156–175. https://doi.org/10.1016/j.mee.2014.10.013
22. Coffer JL, Whitehead MA, Nagesha DK, Mukherjee P, Akkaraju G, Totolici M, Saffie RS, Canham LT (2005) Porous silicon-based scaffolds for tissue engineering and other biomedical applications. Phys Status Solidi A 202 (8):1451–1455. https://doi.org/10.1002/pssa.200461134
23. Wang ST, Liu K, Liu JA, Yu ZTF, Xu XW, Zhao LB, Lee T, Lee EK, Reiss J, Lee YK, Chung LWK, Huang JT, Rettig M, Seligson D, Duraiswamy KN, Shen CKF, Tseng HR (2011) Highly efficient capture of circulating tumor cells by using nanostructured silicon substrates with integrated chaotic micromixers. Angew Chem Int Ed 50(13):3084–3088. https://doi.org/10.1002/anie.201005853
24. Fu JP, Wang YK, Yang MT, Desai RA, Yu XA, Liu ZJ, Chen CS (2010) Mechanical regulation of cell function with geometrically modulated elastomeric substrates. Nat Methods 7 (9):733–U795. https://doi.org/10.1038/nmeth.1487
25. De Clercq E (2005) Recent highlights in the development of new antiviral drugs. Curr Opin Microbiol 8(5):552–560. https://doi.org/10.1016/j.mib.2005.08.010
26. Otterbein LE, Bach FH, Alam J, Soares M, Lu HT, Wysk M, Davis RJ, Flavell RA, Choi AMK (2000) Carbon monoxide has anti-inflammatory effects involving the mitogen-activated protein kinase pathway. Nat Med 6 (4):422–428
27. Mirbagheri M, Adibnia V, Hughes BR, Waldman SD, Banquy X, Hwang DK (2019) Advanced cell culture platforms: a growing quest for emulating natural tissues. Mater Horiz 6(1):45–71. https://doi.org/10.1039/c8mh00803e
28. Morris NJ, Anderson H, Thibeault B, Vertes A, Powell MJ, Razunguzwa TT (2015) Laser desorption ionization (LDI) silicon nanopost array chips fabricated using deep UV projection lithography and deep reactive ion etching. RSC Adv 5(88):72051–72057. https://doi.org/10.1039/c5ra11875a